Asian Journal of Chemistry; Vol. 38, No. 5 (2026), 1308-1316
ASIAN JOURNAL OF CHEMISTRY
https://doi.org/10.14233/ajchem.2026.35642

Novel Phenyl-Triazolo-Thiadiazole Derivatives: Synthesis, Computational Insights and Anti-inflammatory Potential

NILESH A. KARANDE[1], VIKESH V. KUKADE[1,*], LALIT G. RATHI[1], RAJENDRA O. GANJIWALE[1], PRIYANKA D. BANGRE[2], RAJENDRA N. PATIL[3] and DATTATRAYA KATURE[3]

[1]Department of Pharmaceutical Chemistry, Institute of Pharmaceutical Education and Research, Borgaon (Meghe), Wardha-442001, India
[2]Department of Swasthvritta and Yoga, Mahatma Gandhi Ayurved College Hospital and Research Centre, Salod (Hirapur), Wardha-442001, India
[3]Department of Pharmaceutical Chemistry, Delonix Society's Baramati College of Pharmacy, Barhanpur, Baramati-413102, India

*Corresponding author: E-mail: vikeshkukadebcop@gmail.com

Received: 22 January 2026 *Accepted*: 7 April 2026 *Published online*: 4 May 2026 AJC-22356

A novel series of phenyl-triazolo-thiadiazole derivatives (**6a-m**) was designed and synthesised *via* a stepwise synthetic route starting with benzoic acid. The key transformation involved the cyclo-condensation of 4-amino-3-mercapto-5-phenyl-2,4-dihydro-1,2,4-triazole with appropriately substituted benzoic acids to afford the target compounds. All the synthesised derivatives were subjected to comprehensive *in silico* evaluation, like molecular docking, toxicity and density functional theory (DFT) studies. Docking analysis demonstrated that compound **6i** exhibited greater binding affinity (-9.9 kcal/mol) toward the selected inflammatory target when compared with the reference drug mefenamic acid (-8.0 kcal/mol). Toxicological assessment suggested that the synthesised molecules possess acceptable and comparable safety profiles. DFT calculations indicated that compound **6i** displays favourable chemical reactivity, attributed to its moderate electrophilicity index. Furthermore, Molecular dynamics (MD) simulations bear stable protein–ligand interactions for compound **6i**, although minor conformational fluctuations were observed, indicating limited dynamic stability. The anti-inflammatory effectivity of compounds **6a-m** was further validated through *in vivo* rat paw edema experiments, where compound **6i** emerged as the most active candidate, exhibiting the statistically significant activity ($p < 0.01$).

Keywords: Phenyl-triazolo-thiadiazoles, Anti-inflammatory activities, DFT analysis, Molecular docking.

INTRODUCTION

Thiazoles are an important class of heterocyclic compounds and key structural motifs in numerous biologically active and pharmacologically significant molecules. Several therapeutic agents contain the thiazole nucleus including fentiazac and meloxicam (anti-inflammatory), nizatidine (anti-ulcer), sulfathiazole (antimicrobial), ritonavir (antiretroviral) and bleomycin and tiazofurin (antineoplastic) drugs [1-4]. Owing to its privileged pharmacophoric nature, the thiazole ring is widely explored for the design of novel bioactive compounds and exhibits diverse biological activities [5-7].

The chemistry of 1,2,4-triazoles has undergone significant and rapid development in modern heterocyclic research. Literature reports identify the 1,2,4-triazole ring as a key pharmacophoric scaffold with considerable relevance in medicinal chemistry. Derivatives containing this nucleus exhibit a broad spectrum of biological activities including antibacterial, antifungal, antitubercular, and anticancer properties [8-10].

In addition to thiazoles and 1,2,4-triazoles, sulfur containing heterocycles constitute another important class of compounds with considerable synthetic and pharmacological relevance. Numerous derivatives of these sulfur heterocycles have been reported to exhibit diverse biological activities, including antibacterial, antitubercular, antifungal, anticancer, antimycobacterial, diuretic and hypoglycemic properties [11-13]. Among them, mercapto-substituted 1,2,4-triazoles have attracted particular attention because of their dual importance as bioactive molecules and versatile synthetic intermediates. Owing to the presence of a reactive mercapto group, these compounds readily undergo cyclization and condensation reactions to furnish fused heterocyclic systems such as triazolo-

This is an open access journal, and articles are distributed under the terms of the Attribution 4.0 International (CC BY 4.0) License. This license lets others distribute, remix, tweak, and build upon your work, even commercially, as long as they credit the author for the original creation. You must give appropriate credit, provide a link to the license, and indicate if changes were made.

thiadiazoles, triazolothiazepines, triazolothiazines thiazolotriazoles and triazolothiadiazines [14,15].

Notably, 4-amino-3-mercapto-5-phenyl-2,4-dihydro-1,2,4-triazole has emerged as a valuable bifunctional precursor for the synthesis of structurally diverse and pharmacologically significant heterocycles, particularly triazolothiadiazole derivatives. These fused systems have been extensively investigated in medicinal chemistry and have demonstrated promising antimicrobial and anti-inflammatory activities, highlighting their potential for further structural optimization and therapeutic development [16].

Recent advances in heterocyclic and medicinal chemistry have highlighted the strategic importance of halogen substitution in modulating molecular properties. Incorporation of halogen atoms can alter lipophilicity, electronic distribution, metabolic stability, target-binding affinity and is therefore widely employed in the rational design of bioactive molecules [17]. In particular, replacement of hydrogen with halogen substituents has frequently resulted in the enhanced biological activity across diverse heterocyclic systems. Accordingly, the introduction of a chlorophenyl moiety was expected to improve the pharmacological potential of the synthesized compounds, consistent with the reported activity of 1,2,4-triazolo[3,4-*b*][1,3,4]thiadiazole derivatives [18,19].

Non-steroidal anti-inflammatory drugs (NSAIDs) remain among the most widely used agents for the treatment of pain and inflammation. Their therapeutic action primarily arises from inhibition of cyclooxygenase (COX)-mediated prostaglandin biosynthesis. However, the presence of two functionally distinct COX isoforms and the non-selective inhibition exhibited by many conventional NSAIDs are associated with adverse effects, particularly gastrointestinal complications [20,21]. In addition, the predominantly acidic nature of several clinically used NSAIDs contributes to gastric irritation, thereby limiting long-term use.

These limitations have stimulated continued efforts toward the discovery of safer anti-inflammatory agents with improved tolerability. In this regard, fused heterocyclic systems possessing established pharmacological relevance have gained increasing attention. Among them, triazolothiadiazole scaffolds, containing fused triazole and thiadiazole rings, represent promising candidates for anti-inflammatory drug development. Based on these considerations, the present study focuses on the rational design and synthesis of a series of triazolothiadiazole derivatives, followed by systematic evaluation of their anti-inflammatory potential using integrated computational and experimental approaches, with the aim of identifying structurally optimized and safer therapeutic candidates [22,23].

EXPERIMENTAL

All reagents were purchased from Merck (India) and Loba Chemicals (India) and used as received. Solvents were freshly distilled prior to use. Reaction progress and purity was assessed by TLC on silica gel 60 F_{254} plates using chloroform: ethanol (7:3, v/v) as the mobile phase. Infrared spectra were recorded on a Shimadzu spectrometer and NMR spectra were obtained on a Bruker automated spectrometer using DMSO-d_6 as the solvent. Mass spectra were acquired using a Micromass Q-TOF mass spectrometer, while elemental analyses were performed with a Perkin-Elmer CHNS/O analyzer (Series II, USA).

Synthesis of 4-amino-3-mercapto-5-phenyl-2,4-dihydro-1,2,4-triazole (5): Benzoic acid (**1**, 0.246 mol) was esterified with methanol (2.5 mol) in the presence of conc. H_2SO_4 (2.7 mL) under reflux to afford methyl benzoate (**2**) in 50% yield. Compound **2** (0.073 mol) was subsequently treated with hydrazine hydrate (0.21 mol) in ethanol to obtain benzohydrazide (**3**) in 50% yield. Benzohydrazide (**3**) (0.01 mol) was dissolved in methanol (10 mL), cooled to 0-5 ºC and reacted with KOH (2 g) and CS_2 to furnish the corresponding potassium dithiocarbazate intermediate (**4**) in 78% yield. Refluxing compound **4** (0.01 mol) with hydrazine hydrate (0.01 mol) for 4-6 h resulted in cyclization with evolution of H_2S. The reaction mixture was then acidified, and the resulting precipitate was collected, washed with cold water and recrystallized from aqueous methanol to yield 4-amino-3-mercapto-5-phenyl-2,4-dihydro-1,2,4-triazole (**5**) as a white solid. Yield 48%; m.p.: 195-198 ºC (lit. 211-215 ºC); FTIR (KBr, ν_{max}, cm^{-1}): 3120 (N–H), 3050 (Ar. H), 2960 (Ar. H), 2550 (S-H), 1650 (C=N), 1600 (C=C), 1475 (C=C), 1120 (C–N), 640 (C–S); ^{1}H NMR, 400 MHz, DMSO-d_6: δ 5.70 (s, 2H, amine), 7.81-7.61 (d, 2H, *J* = 8.24 Hz, benzene), 8.19-7.88 (t, *J* = 8.13 Hz, 3H, benzene), 13.90 (s, 1H, Ar. C–S-H); ^{13}C NMR (125 MHz, DMSO-d_6, δ ppm): 126.43, 128.31, 128.78, 129.04, 131.94, 135.80, 148.38, 164.74; LC-MS, *m/z*, %: 193.06, M+1, 9.8%.

Synthesis of phenyl-triazolo-thiadiazole derivatives (6a-m): Compound **5** (0.01 mol) and the appropriate substituted benzoic acid (0.01 mol) were dissolved in $POCl_3$ (10 mL) and refluxed for 7-8 h. After completion. The mixture was poured over crushed ice and neutralised with aqueous sodium bicarbonate. The resulting phenyl-triazolo-thiadiazole derivatives (**6a-m**) were collected by filtration, washed with water, dried and recrystallised using hot ethanol (**Scheme-I**).

3,6-Diphenyl-[1,2,4]triazolo[3,4-*b*][1,3,4]thiadiazole (6a): Colour: white, yield: 88%, m.p.: 112-114 ºC; Elemental analysis of $C_{15}H_{10}N_4S$ (m.w. 278.33): calcd. (found) %: C, 64.73 (64.77); H, 3.62 (3.68); N, 20.13 (20.10); S, 11.52 (11.48); FTIR (KBr, ν_{max}, cm^{-1}): 2910 (Ar. H), 1690 (C=N), 1600 (C=C), 1475 (C=C), 1360 (C–N), 1170 (N–N), 760 (C–S); ^{1}H NMR (400 MHz, DMSO-d_6, δ ppm): 8.46-8.32 (d, *J* = 8.17 Hz, 2H, phenyl-triazolothiadiazoles), 8.26-7.96 (d, *J* = 8.44 Hz, 2H, phenyl-triazolothiadiazoles), 7.83-7.59 (t, *J* = 7.98 Hz, 3H, benzene), 7.46-7.35 (t, *J* = 8.11 Hz, 3H, benzene); ^{13}C NMR (125 MHz, DMSO-d_6, δ ppm): 127.17, 127.56, 128.27, 129.33, 129.56, 129.82, 129.99, 130.56, 130.84, 130.92, 131.56, 133.48, 149.64, 154.12, 167.11; LC-MS, *m/z*, %: 293.21, M+1, 20.10.

6-(2-Chlorophenyl)-3-phenyl-[1,2,4]triazolo[3,4-*b*]-[1,3,4]thiadiazole (6b): Colour: white, yield: 82%, m.p.: 127-129 ºC; Elemental analysis of $C_{15}H_9N_4SCl$ (m.w. 312.78): calcd. (found) %: C, 57.60 (57.63); H, 2.90 (2.91); N, 17.91 (17.93); S, 10.25 (10.28); FTIR (KBr, ν_{max}, cm^{-1}): 3100 (Ar. H), 1680 (C=N), 1600 (C=C), 1475 (C=C), 1400 (C–N), 740 (C–Cl), 830 (C–S); ^{1}H NMR (400 MHz, DMSO-d_6, δ ppm): 8.46-8.32 (d, *J* = 8.09 Hz, 2H, phenyl-triazolothiadiazoles), 8.26-7.96 (t, *J* = 8.15 Hz, 2H, phenyl-triazolothiadiazoles), 7.83-7.64 (d, *J* = 7.89 Hz, 2H, benzene), 7.59-7.35 (t, *J* = 8.31

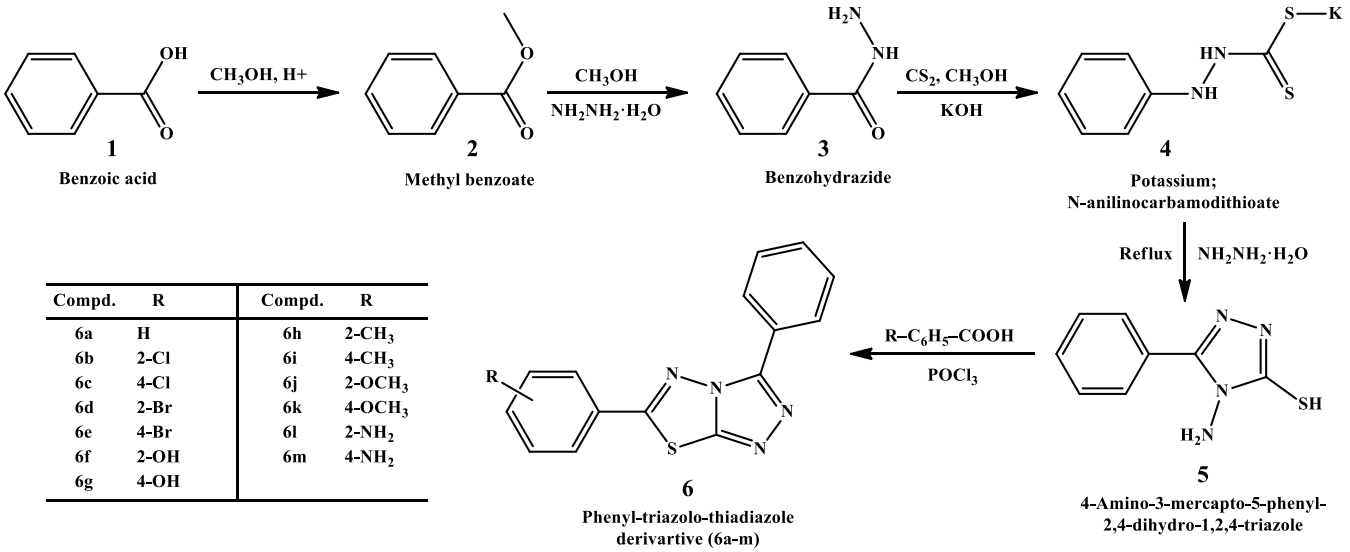

Compd.	R	Compd.	R
6a	H	6h	2-CH_3
6b	2-Cl	6i	4-CH_3
6c	4-Cl	6j	2-OCH_3
6d	2-Br	6k	4-OCH_3
6e	4-Br	6l	2-NH_2
6f	2-OH	6m	4-NH_2
6g	4-OH		

Scheme-I: Synthesis of phenyl-triazolo-thiadiazole derivatives (**6a-m**)

Hz, 3H, benzene); ^{13}C NMR (125 MHz, DMSO-d_6, δ ppm): 127.12, 127.44, 127.56, 128.27, 129.33, 129.56, 129.82, 130.56, 130.84, 131.56, 132.48, 148.78, 153.12, 167.11, 174.56; LC-MS, *m/z*, %: 313.48, M+1, 23.1.

6-(4-Chlorophenyl)-3-phenyl-[1,2,4]triazolo[3,4-*b*]-[1,3,4]-thiadiazole (6c): Colour: white, yield: 79%, m.p.: 123-125 ºC; Elemental analysis of $C_{15}H_9N_4SCl$ (m.w. 312.78): calcd. (found) %: C, 57.62 (57.64); H, 2.96 (2.95); N, 17.95 (17.96); S, 10.23 (10.26); FTIR (KBr, ν_{max}, cm^{-1}): 3110 (Ar. H *str.*), 1680 (C=N *str.*), 1475 (C=C *str.*), 1320 (C–N *str.*), 680 (C–Cl *str.*), 840 (C–S *str.*); ^{1}H NMR (400 MHz, DMSO-d_6, δ ppm): 8.46-8.22 (d, *J* = 8.11 Hz, 2H, phenyl-triazolothia-diazoles), 8.16-7.81 (t, *J* = 8.07 Hz, 2H, phenyl-triazolothia-diazoles), 7.76-7.62 (d, *J* = 7.77 Hz, 2H, benzene), 7.55-7.45 (t, *J* = 8.13 Hz, 3H, benzene); ^{13}C NMR, (125 MHz, DMSO-d_6, δ ppm): 127.17,127.56, 128.27, 128.73, 129.16, 129.42, 129.69, 129.86, 130.84, 131.42, 131.56, 134.48, 143.84, 154.78, 167.14; LC-MS, *m/z*, %: 314.11, M+1, 21.1.

6-(2-Bromophenyl)-3-phenyl-[1,2,4]triazolo[3,4-*b*]-[1,3,4]thiadiazole (6d): Colour: yellow, yield: 66%, m.p.: 120-122 ºC; Elemental analysis of $C_{15}H_9N_4SBr$ (m.w. 357.23): calcd. (found) %: C, 50.43 (50.48); H, 2.59 (2.61); N, 15.39 (15.41); S, 9.24 (9.27); FTIR (KBr, ν_{max}, cm^{-1}): 3130 (Ar–H *str.*), 1680 (C=N *str.*), 1590 (C=C *str.*), 1430 (C=C *str.*), 1350 (C–N *str.*), 760 (C–S *str.*), 620 (C-Br *str.*); ^{1}H NMR (400 MHz, DMSO-d_6, δ ppm): 8.43-8.24 (d, *J* = 8.06 Hz, 2H, phenyl-triazolothiadiazoles), 7.94-7.74 (t, *J* = 8.15 Hz, 2H, phenyl-triazolothiadiazoles), 7.67-7.53 (d, *J* = 7.81 Hz, 2H, benzene), 7.45-7.33 (t, *J* = 8.11 Hz, 3H, benzene); ^{13}C NMR (125 MHz, DMSO-d_6, δ ppm): 127.33, 127.49, 127.56, 128.29, 129.43, 129.76, 129.82, 130.56, 130.84, 131.86, 132.78, 147.78, 154.75, 166.89, 176.12; LC-MS, *m/z*, %: 358.19, M+1, 28.1.

6-(4-Bromophenyl)-3-phenyl-[1,2,4]triazolo[3,4-*b*]-[1,3,4]thiadiazole (6e): Colour: yellow, yield: 69%, m.p.: 112-114 ºC; Elemental analysis of $C_{15}H_9N_4SBr$ (m.w. 357.23): calcd. (found) %: C, 50.47 (50.49); H, 2.54 (2.58); N, 15.43 (15.45); S, 9.27 (9.33); FTIR (KBr, ν_{max}, cm^{-1}): 3110 (Ar–H *str.*), 1690 (C=N *str.*), 1590 (C=C *str.*), 1475 (C=C *str.*), 1280 (C–N), 640 (C–S *str.*), 840 (C-Br *str.*); ^{1}H NMR (400 MHz, DMSO-d_6, δ ppm): 8.38-8.21 (d, *J* = 8.19 Hz, 2H, phenyl-triazolothiadiazoles), 8.15-7.86 (t, *J* = 8.25 Hz, 2H, phenyl-triazolothiadiazoles), 7.78-7.65 (d, *J* = 7.65 Hz, 2H, benzene), 7.58-7.45 (t, *J* = 8.52 Hz, 3H, benzene); ^{13}C NMR, (125 MHz, DMSO-d_6, δ ppm): 127.44, 127.56, 128.54, 128.73, 129.20, 129.43, 129.70, 129.87, 130.33, 13126, 131.66, 134.12, 143.64, 154.77, 167.44; LC-MS, *m/z*, %: 358.11, M+1, 19.1.

2-(3-Phenyl-[1,2,4]triazolo[3,4-*b*][1,3,4]thiadiazol-6-yl)phenol (6f): Colour: white, yield: 82%, m.p.: 146-148 ºC; Elemental analysis of $C_{15}H_{10}N_4OS$ (m.w. 294.33): calcd. (found) %: C, 63.95 (63.98); H, 5.04 (5.09); N, 18.27 (18.31); S, 10.89 (10.85); FTIR (KBr, ν_{max}, cm^{-1}): 3440 (O–H *str.*), 3110 (Ar–H *str.*), 1680 (C=N *str.*), 1590 (C=C *str.*), 1430 (C=C *str.*), 1320 (C–N *str.*), 1180 (C–O *str.*), 770 (C–S *str.*); ^{1}H NMR (400 MHz, DMSO-d_6, δ ppm): 9.68-9.60 (s, 1H, Hydroxy), 8.52-8.23 (d, *J* = 8.26 Hz, 2H, benzene), 7.98-7.69 (t, *J* = 8.23 Hz, 2H, benzene), 7.62-7.42 (d, *J* = 8.09 Hz, 2H, phenyl-triazolothiadiazoles), 7.35-7.19 (t, *J* = 8.12 Hz, 3H, phenyl-triazolothiadiazoles); ^{13}C NMR (125 MHz, DMSO-d_6, δ ppm): 127.28, 127.67, 127.88, 128.17, 129.43, 129.66, 129.82, 130.56, 130.87, 131.15, 132.48, 147.88, 154.55, 166.12, 175.56; LC-MS, *m/z*, %: 295.12, M+1, 32.1.

4-(3-Phenyl-[1,2,4]triazolo[3,4-*b*][1,3,4]thiadiazol-6-yl)phenol (6g): Colour: white, yield: 83%, m.p.: 150-152 ºC; Elemental analysis of $C_{15}H_{10}N_4OS$ (m.w. 294.33): calcd. (found) %: C, 64.02 (64.07); H, 5.35 (5.38); N, 19.27 (19.25); S, 10.78 (10.74); FTIR (KBr, ν_{max}, cm^{-1}): 3390 (O–H *str.*), 3150 (Ar–H *str.*), 1610 (C=N *str.*), 1610 (C=C *str.*), 1475 (C=C *str.*), 1380 (C–N *str.*), 1240 (C–O *str.*), 760 (C–S *str.*); ^{1}H NMR (400 MHz, DMSO-d_6, δ ppm): 9.79-9.72 (s, 1H, Hydroxy), 8.48-8.26 (d, *J* = 8.13 Hz, 2H, benzene), 7.98-7.71 (t, *J* = 8.61 Hz, 2H, benzene), 7.61-7.47 (d, *J* = 8.33Hz, 2H, phenyl-triazolothiadiazoles), 7.36-7.11 (t, *J* = 8.56 Hz, 3H, phenyl-triazolothiadiazoles); ^{13}C NMR (125 MHz, DMSO-d_6, δ ppm): 127.24, 127.67, 138.25, 128.60, 129.22, 129.43,

129.73, 129.88, 130.35, 131.26, 131.66, 134.14, 143.74, 154.84, 167.47; LC-MS, *m/z*, %: 295.14, M+1, 32.1.

3-Phenyl-6-(*o*-tolyl)-[1,2,4]triazolo[3,4-*b*][1,3,4]thiadiazole (6h): Colour: brown, yield: 74%, m.p.: 110-112 ºC; Elemental analysis of $C_{16}H_{12}N_4S$ (m.w. 292.36): calcd. (found) %: C, 59.89 (59.92); H, 4.40 (4.41); N, 18.17 (18.24); S, 10.83 (10.79); FTIR (KBr, ν_{max}, cm^{-1}): 3240 (C–H aromatic *str.*), 3140 (C–H of CH_3 *str.*), 1620 (C=N *str.*), 1455 (C=C), 1340 (C–N), 740 (C–S *str.*); ^{1}H NMR (400 MHz, DMSO-d_6, δ ppm): 8.41-7.91 (d, *J* = 8.41 Hz, 2H, phenyl-triazolothiadiazoles), 7.86-7.62 (t, *J* = 8.25 Hz, 2H, phenyl-triazolothiadiazoles), 7.56-7.35 (d, *J* = 8.41 Hz, 2H, benzene), 7.22-7.12 (t, *J* = 8.23 Hz, 3H, benzene), 2.63 (s, 3H, methyl); ^{13}C NMR, 125 (400 MHz, DMSO-d_6, δ ppm): 18.63, 125.57, 127.88, 128.17, 128.63, 129.46, 129.52, 130.16, 130.87, 131.15, 132.43, 133.15, 151.11, 156.55, 167.41, 177.71; LC-MS, *m/z*, %: 293.14, M+1, 19.0.

3-Phenyl-6-(*p*-tolyl)-[1,2,4]triazolo[3,4-*b*][1,3,4]thiadiazole (6i): Colour: brown, yield: 68%, m.p.: 116-118 ºC; Elemental analysis of $C_{16}H_{12}N_4S$ (m.w. 292.36): calcd. (found) %: C, 58.89 (58.86); H, 5.40 (5.43); N, 17.93 (17.89); S, 11.13 (11.15); FTIR (KBr, ν_{max}, cm^{-1}): 3250 (C–H aromatic *str.*), 3140 (C–H of CH_3 *str.*), 1610 (C=N *str.*), 1450 (C=C), 1350 (C–N), 750 (C–S *str.*); ^{1}H NMR (400 MHz, DMSO-d_6, δ ppm): 8.44-7.92 (d, *J* = 8.46 Hz, 2H, phenyl-triazolothiadiazoles), 7.85-7.64 (t, *J* = 8.18 Hz, 2H, phenyl-triazolothiadiazoles), 7.55-7.36 (d, *J* = 8.19 Hz, 2H, benzene), 7.22-7.14 (t, *J* = 8.77 Hz, 3H, benzene), 2.74 (s, 3H, methyl); ^{13}C NMR (125 MHz, DMSO-d_6, δ ppm): 19.81, 127.25, 127.76, 128.39, 128.73, 129.21, 129.59, 129.68, 129.87, 130.61, 131.26, 131.59, 134.29, 143.53, 154.84, 167.86; LC-MS, *m/z*, %: 293.32, M+1, 18.0.

6-(2-Methoxyphenyl)-3-phenyl-[1,2,4]triazolo[3,4-*b*]-[1,3,4]thiadiazole (6j): Colour: white, yield: 69%, m.p.: 156-158 ºC; Elemental analysis of $C_{16}H_{12}N_4OS$ (m.w. 308.36): calcd. (found) %: C, 60.06 (60.11); H, 4.72 (4.60); N, 23.52 (23.48); S, 11.86 (11.82); FTIR (KBr, ν_{max}, cm^{-1}): 3320 (C–H aromatic *str.*), 2920 (C–H of CH_3 *str.*), 1610 (C=N *str.*), 1475 (C=C), 1240 (C–O), 1120 (C–N), 750 (C–S *str.*); ^{1}H NMR (400 MHz, DMSO-d_6, δ ppm): 8.38-7.93 (d, *J* = 8.33 Hz, 2H, phenyl-triazolothiadiazoles), 7.88-7.67 (t, *J* = 8.93 Hz, 2H, phenyl-triazolothiadiazoles), 7.56-7.31(d, *J* = 8.15 Hz, 2H, benzene),7.26-7.16 (t, *J* = 8.34 Hz, 3H, benzene), 4.21 (s, 3H, methoxy); ^{13}C NMR (125 MHz, DMSO-d_6, δ ppm): 56.29, 125.55, 127.84, 128.22, 128.63, 129.44, 129.52, 130.16, 130.72, 131.15, 132.40, 133.41, 151.11, 156.49, 167.15, 177.77; LC-MS, *m/z*, %: 309.23, M+1, 22.40.

6-(4-Methoxyphenyl)-3-phenyl-[1,2,4]triazolo[3,4-*b*]-[1,3,4]thiadiazole (6k): Colour: white, yield: 71%, m.p.: 162-164 ºC; Elemental analysis of $C_{16}H_{12}N_4OS$ (m.w. 308.36): calcd. (found) %: C, 60.26 (60.23); H, 4.86 (4.82); N, 23.64 (23.61); S, 11.76 (11.73); FTIR (KBr, ν_{max}, cm^{-1}): 3260 (C–H aromatic *str.*), 3120 (C–H of CH_3 *str.*), 1630 (C=N *str.*), 1240 (C–O), 1100 (C–N), 750 (C–S *str.*); ^{1}H NMR (400 (400 MHz, DMSO-d_6, δ ppm): 8.34-7.91 (d, *J* = 8.82 Hz, 2H, phenyl-triazolothiadiazoles), 7.87-7.61 (t, *J* = 8.33 Hz, 2H, phenyl-triazolothiadiazoles), 7.54-7.33 (d, *J* = 8.59 Hz, 2H, benzene), 7.25-7.17 (t, *J* = 8.89 Hz, 3H, benzene), 4.28 (s, 3H, methoxy); ^{13}C NMR (125 MHz, DMSO-d_6, δ ppm): 55.86, 123.25, 125.76, 127.39, 128.73, 129.21, 129.59, 129.68, 129.87, 130.61, 131.26, 131.49, 134.86, 143.72, 154.84, 167.25; LC-MS, *m/z*, %: 309.22, M+1, 18.61.

2-(3-Phenyl-[1,2,4]triazolo[3,4-*b*][1,3,4]thiadiazol-6-yl)aniline (6l): Colour: white, yield: 77%, m.p.: 123-125 ºC; Elemental analysis of $C_{15}H_{11}N_5S$ (m.w. 293.35): calcd. (found) %: C, 58.55 (58.51); H, 4.16 (4.21); N, 19.66 (19.61); S, 10.86 (10.82); FTIR (KBr, ν_{max}, cm^{-1}): 3380 (N–H *str.*), 3320 (C–H aromatic *str.*), 1610 (C=N *str.*), 1475 (C=C *str.*), 1120 (C–N *str.*), 830 (C–S); ^{1}H NMR (400 MHz, DMSO-d_6, δ ppm): 8.37-7.93 (d, *J* = 8.26 Hz, 2H, benzene), 7.88-7.61 (t, *J* = 8.36 Hz, 2H, benzene), 7.47-7.28 (d, *J* = 8.91 Hz, 2H, phenyl-triazolothiadiazoles), 7.19-6.91 (t, *J* = 8.52 Hz, 3H, phenyl-triazolothiadiazoles), 5.53 (s, 2H, amino); ^{13}C NMR (125 (400 MHz, DMSO-d_6, δ ppm): 123.28, 125.57, 127.88, 128.17, 128.53, 129.46, 129.82, 130.16, 130.87, 131.15, 132.43, 151.11, 156.55, 167.12, 177.56; LC-MS, *m/z*, %: 294.46, M+2, 50.23%.

4-(3-Phenyl-[1,2,4]triazolo[3,4-*b*][1,3,4]thiadiazol-6-yl)aniline (6m): Colour: white, yield: 75%, m.p.: 128-130 ºC; Elemental analysis of $C_{15}H_{11}N_5S$ (m.w. 293.35): calcd. (found) %: C, 58.63 (58.65); H, 4.07 (4.11); N, 19.06 (19.10); S, 10.77 (10.78); FTIR (KBr, ν_{max}, cm^{-1}): 3380 (N–H *str.*), 3310 (C–H aromatic *str.*), 1610 (C=N *str.*), 1475 (C=C *str.*), 1120 (C–N *str.*), 840 (C–S); ^{1}H NMR (400 MHz, DMSO-d_6, δ ppm): 8.31-7.89 (d, *J* = 8.53 Hz, 2H, benzene), 7.79-7.59 (t, *J* = 8.69 Hz, 2H, benzene), 7.48-7.29 (d, *J* = 8.38 Hz, 2H, phenyl-triazolothiadiazoles), 7.18-6.93 (t, *J* = 8.59 Hz, 3H, phenyl-triazolothiadiazoles), 5.47 (s, 2H, amino); ^{13}C NMR (125 (400 MHz, DMSO-d_6, δ ppm): 123.59, 125.58, 126.98, 127.57, 128.26, 129.16, 129.82, 130.22, 130.87, 131.15, 132.43, 151.15, 156.17, 167.52, 177.19; LC-MS, *m/z*, %: 294.46, M+2, 51.28.

Molecular docking: Molecular docking was carried out by Schrödinger Maestro 2023 (12.5) to evaluate ligand binding to COX-II (PDB ID: 5IKR, Chain B). The protein was prepared by Protein Preparation Wizard; water and cofactors removed. The active pocket was defined and the docking grid was generated based on pharmacophore alignment. Binding affinities were calculated, with ligand **6i** exhibiting the uppermost docking score of –9.9 kcal/mol.

Toxicity prediction: *In silico* toxicity assessment was performed using ProTox3.0. All ligands exhibited a predicted LD_{50} of 800 mg/kg, classifying them as Class IV on the GHS scale, indicative of low toxicity. The predictions suggested comparable hepatotoxicity and immunotoxicity risks across the ligands, which displayed a safer profile relative to mefenamic acid.

Density functional theory (DFT) analysis: DFT were performed for all 13 ligands using GaussView 5.0 to evaluate their electronic properties. Key parameters, including HOMO, LUMO, energy gap and electrophilicity, were analysed. Ligand **6i** exhibited the highest docking affinity, with a DFT profile indicating a soft ligand with moderate electrophilicity, high chemical reactivity, structural stability and favourable drug-like characteristics, identifying it as the most promising candidate for further study.

Molecular dynamics simulation: A 100 ns MD simulation of the COX-II-ligand **6i** complex was conducted using Desmond software. The system was solvated and simulated under NPT conditions at 310 K and 1 atm. The complex exhibited stable RMSD, hydrogen-bonding and hydrophobic-interactions during the simulation. While ligand **6i** maintained stable binding, DFT analysis suggested high reactivity with potential implications for long-term stability.

Acute toxicity studies: Acute oral toxicity was evaluated following OECD guidelines 420 (fixed dose procedure) [24]. Female Wistar albino rats (160-225 g) were randomly assigned to groups of three and housed in polypropylene cages under standard laboratory conditions. Animals were housed for 1 week before dosing to allow adaptation. The test compounds were administered orally as suspensions in 0.5% methyl cellulose at a starting dose of 50 mg/kg body weight by single gavage. Animals were closely observed for the first 30 min, intermittently for 6 h and daily for 14 days. The parameters including mortality, clinical signs, behavioural changes, food intake and body weight were recorded. No mortality, abnormal behaviour or significant body weight changes were observed, indicating an LD_{50} greater than 50 mg/kg. Based on these results, a safe working dose of 10 mg/kg body weight was selected for the evaluation of anti-inflammatory activity. The study was approved by the Institutional Animal Ethics Committee (IAEC; Reg. No. 535/PO/ReRcBt/S/02/CPCSEA; Proposal No. 535/PO/ReRcBt/S/02/CPCSEA/IPER/IAEC/2025-26/02).

***In vivo* evaluation of anti-inflammatory activity:** The anti-inflammatory activity of compounds **6a-m** was assessed in Wistar albino rats (170-260 g) using the carrageenan-induced paw edema model as described by Winter *et al.* [25]. Mefenamic acid (1.5 mg/kg, p.o.) served as the standard. Animals maintained under controlled laboratory conditions were randomly divided into fourteen groups (n = 6). Test compounds were administered orally at 10 mg/kg as a 2% gum acacia suspension. Acute inflammation was induced 1 h later by sub-plantar injection of 0.1 mL of 1% carrageenan into the left hind paw. Paw volume was measured at baseline and at selected time intervals using a digital plethysmometer and anti-inflammatory activity was expressed as percentage inhibition of edema relative to the control.

$$\text{Edema inhibition (\%)} = 100 - \left(\frac{V_{test}}{V_{control}}\right) \times 100$$

where: V= amount of paw edema (in both the control and the test conditions).

RESULTS AND DISCUSSION

The phenyl-triazolo-thiadiazole derivatives (**6a-m**) were synthesised through a multistep route starting from benzoic acid. Potassium *N*-anilinocarbamodithioate (**4**) was prepared from benzoic acid according to reported methods [19,20]. Refluxing compound **4** with hydrazine hydrate yielded 4-amino-3-mercapto-5-phenyl-2,4-di-hydro-1,2,4-triazole (**5**). The target derivatives **6a-m** were then obtained by reacting compound **5** with various substituted benzoic acids in $POCl_3$ under reflux. The structural characterisation was carried out using ^1H and ^{13}C NMR, FTIR, mass spectrometry and elemental analysis.

Molecular docking: Molecular docking were performed for synthesised phenyl-triazolo-thiadiazole derivatives (**6a-m**) and compared with the standard ligand. Among the series, compound **6i** exhibited maximal affinity (-9.9 kcal/mol), followed by compounds **6a, 6g** and **6l** (-9.6 kcal/mol). Compounds **6b**, **6c** and **6h** also demonstrated favourable binding energies (-9.5 kcal/mol), exceeding that of the reference drug mefenamic acid (-8.0 kcal/mol) (Table-1). Hence, based on results, it is observed that several derivatives exhibited stronger binding than the standard, suggesting their potential as more effective inhibitors. The docking images are shown in Fig. 1.

TABLE-1
TOXICITY AND BINDING AFFINITIES DATA OF THE SYNTHETIC COMPOUNDS (**6a-m**)

Ligand	Toxicity dose predicted LD50 (mg/kg)	Toxicity class	Binding affinity (kcal/mol)
6a	800	4	-9.6
6b	800	4	-9.5
6c	800	4	-9.5
6d	800	4	-9.4
6e	800	4	-9.4
6f	800	4	-9.0
6g	800	4	-9.6
6h	800	4	-9.5
6i	800	4	-9.9
6j	800	4	-8.6
6k	800	4	-9.4
6l	800	4	-9.6
6m	800	4	-9.4
Standard	525	4	8.0

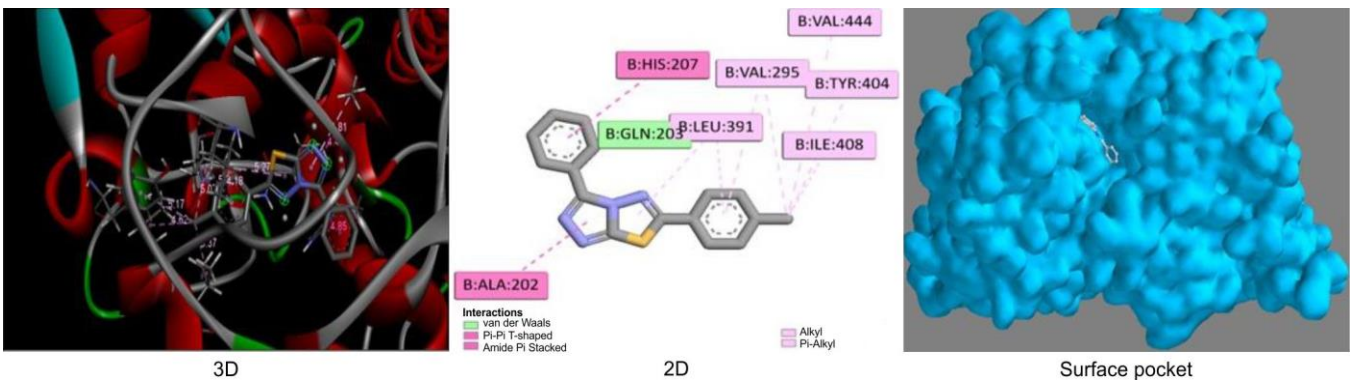

Fig. 1. Visualisations of docked molecule **6i**

Toxicity estimation: All 13 docked ligands were further assessed for predicted toxicity, covering key safety parameters. The evaluation focused on estimated LD_{50} values and toxicity classification, as summarised in Table-1, to identify compounds with acceptable safety profiles. The ligands showed comparable predicted LD_{50} values and toxicity classes; therefore, final selection was based on a combined consideration of docking scores and toxicity predictions. On this basis, ligand **6i** proved most promising, demonstrating a favourable balance between binding affinity and predicted safety and was selected for further investigation.

DFT studies: DFT were performed to examine the electronic properties, stability and reactivity of the phenyl-triazolo-thiadiazole derivatives **(6a-m)**, ligand **6i** exhibits the most favourable electronic profile for electron-transfer processes. It possesses a high dipole moment (6.4320 Debye) and a narrow HOMO-LUMO energy gap (ΔE = -0.00569 a.u.; E_{HOMO} = -0.03160 a.u., E_{LUMO} = -0.03729 a.u.), indicating high softness and reactivity. Its ionisation potential (0.85988 eV) and electron affinity (1.014713 eV) suggest balanced electron-donating and electron-accepting capabilities, while its electrochemical potential (-0.9373 eV) and electronegativity (0.937296 eV) further support its efficiency in charge-transfer mechanisms. The electrophilicity (-5.67402 eV), hardness (-0.07742 eV) and softness (-12.9172 eV) values confirm **6i** as the most reactive yet sufficiently stable ligand in the series. Other ligands, such as **6j** and **6k**, exhibit higher electrophilicity but reduced softness, implying comparatively lower adaptability in electron-transfer reactions. Ligands **6a** and **6d** show greater softness but lower electrophilicity, indicating a distinct reactivity pattern. Ligands **6b** and **6c** demonstrate moderate reactivity, yet their higher ionisation potential and electron affinity reduce their efficiency in comparison to **6i**. The findings are depicted in Fig. 2 and summarised in Table-2.

MD simulation: Protein–ligand complex stability of compound **6i** was evaluated using MD simulation. RMSD analysis indicated that the ligand remained firmly bound with minimal positional deviation, while the protein backbone achieved stability within 1-3 Å. RMSF analysis present expected flexibility in loop and terminal residues, with negligible fluctuations at ligand-interacting residues, indicating stable binding. Secondary structure element (SSE) analysis revealed a consistent structural composition (helix 33.80%, strand 4.11%, total SSE 37.91%), confirming preservation of protein integrity throughout the simulation. Interaction analysis identified persistent hydrogen bonds, water-mediated interactions, ionic and hydrophobic contacts, with key residues participating in more than 70% of simulation frames. Ligand–protein contact maps confirmed sustained multivalent interactions, while torsional analysis demonstrated limited ligand flexibility

TABLE-2
DFT CALCULATIONS (QUANTUM CHEMICAL DESCRIPTORS) OF THE SYNTHESISED DERIVATIVES (**6a-m**)

Ligand	Dipole moment (Debye)	HOMO (a.u.)	LUMO (a.u.)	Energy Gap (ΔE_{Gap})	Ionisation Potential (eV)	Electron affinity (eV)	Electronegativity χ (eV)	Electrochemical potential μ (eV)	Hardness η (eV)
6a	5.3784	-0.04288	-0.05027	0.13721	5.834	2.101	1.26737	-1.26737	1.867
6b	2.5137	-0.02124	-0.04610	0.12996	5.835	2.299	0.916207	-0.91621	1.768
6c	5.5018	-0.05245	-0.06612	0.13383	5.936	2.294	1.613227	-1.61323	1.821
6d	4.3630	-0.02055	-0.02276	0.13553	6.048	2.360	0.589263	-0.58926	1.844
6e	5.6318	-0.04061	-0.05211	0.14101	5.776	1.939	1.26152	-1.26152	1.919
6f	2.2983	-0.01599	-0.05171	0.13845	5.766	1.998	0.921105	-0.92111	1.884
6g	1.0751	-0.02223	-0.05544	0.14713	5.557	1.554	1.056754	-1.05675	2.002
6h	1.5262	-0.01615	-0.09800	0.13552	5.832	2.144	1.55309	-1.55309	1.844
6i	6.4320	-0.03160	-0.03729	0.13907	5.789	2.005	0.937296	-0.9373	1.892
6j	5.8368	-0.08039	-0.21223	0.13594	5.659	1.960	3.981298	-3.9813	1.850
6k	6.1256	-0.08070	-0.21979	0.14091	5.767	1.932	4.088375	-4.08837	1.917
6l	1.2217	-0.01002	-0.05975	0.07603	5.844	3.775	0.949269	-0.94927	1.034
6m	1.1274	-0.02641	-0.05552	0.09079	6.163	3.692	1.114714	-1.11471	1.235

Ligand	Softness, S (eV)	Electrophilicity, ω (eV)	Inference
6a	0.536	4.216	Very soft, high electrophilicity = highly reactive & good electron-acceptor.
6b	0.566	4.677	Moderately soft; moderate electrophilicity = moderately reactive ligand.
6c	0.549	4.651	Soft ligand with high electrophilicity = strong electrophilic reactivity.
6d	0.542	4.792	Extremely soft (very low hardness) = highly reactive and easily polarised.
6e	0.521	3.878	Soft ligand; good electrophile = favourable for charge-transfer interactions.
6f	0.531	4.000	Moderately soft; moderate electrophilicity = balanced reactivity.
6g	0.500	3.158	Moderately soft; moderate electrophilicity = stable but still reactive.
6h	0.542	4.313	High electron affinity & high χ = strong electron-acceptor; high electrophilic strength.
6i	0.529	4.013	Soft ligand with moderate electrophilicity = good chemical reactivity.
6j	0.541	3.924	Very high electrophilicity & very soft = highly reactive and strong electrophile.
6k	0.522	3.865	Most electrophilic ligand = strongest electron-acceptor; very highly reactive.
6l	0.967	11.180	Moderately soft; lower electrophilicity = comparatively less reactive.
6m	0.810	9.827	Moderately soft and moderately electrophilic = intermediate reactivity.

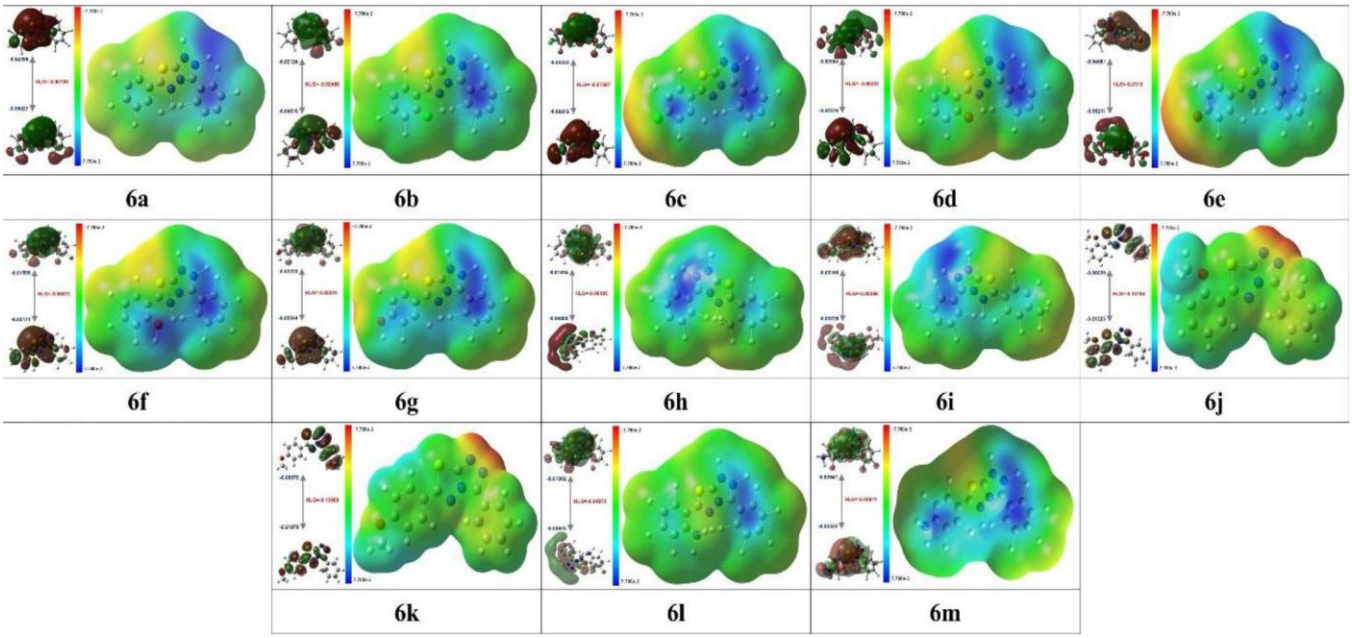

Fig. 2. Visualisations of DFT Analysis (HOMO-LUMO) of synthesised derivatives (**6a-m**)

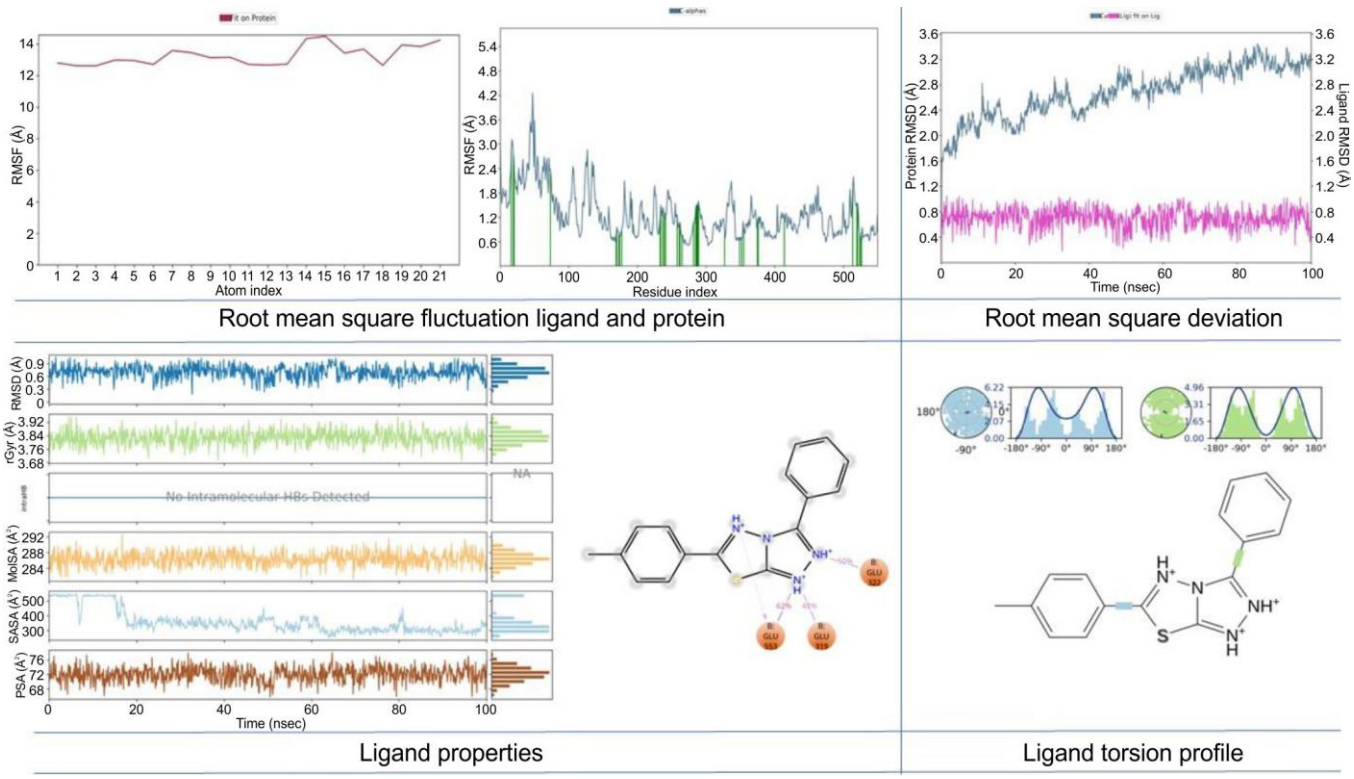

Fig. 3. Visualisations of molecular dynamics simulation of molecule **6i**

consistent with docking poses (Fig. 3). In addition, ligand parameters such as rGyr, MolSA, SASA, PSA and intramolecular hydrogen bonds remained stable throughout the simulation, supporting the stability of the protein–ligand complex.

Anti-inflammatory activity: The anti-inflammatory activity of compounds **6a-m** were statistically analysed using one-way ANOVA followed by Dunnett's test. Among the synthesised derivatives, compound **6i** exhibited a highly significant anti-inflammatory effect ($p < 0.01$), whereas compound **6a** showed a significant response ($p < 0.05$). In contrast, compound **6c** displayed relatively weak activity ($p > 0.05$). Among all tested compounds, **6i** produced the highest inhibition (59.22%) of carrageenan-induced paw edema after 4 h. Although the activity of compound **6i** was comparable to that of the reference drug used in the study, the result indicates that the phenyl-triazolo-thiadiazole scaffold possesses promising anti-inflammatory potential. The enhanced activity of compound **6i** may be attributed to the presence of the electron-

TABLE-3
ANTI-INFLAMMATORY ACTIVITY DATA OF THE SYNTHESISED DERIVATIVES (**6a-m**)

Compound	Dose (mg/kg, p.o.)	Mean paw edema volume after hour[a]				% edema inhibition after hour			
		1	2	3	4	1	2	3	4
Control	10 mL/kg	0.181 ± 0.0023	0.342 ± 0.0046	0.578 ± 0.0065	0.659 ± 0.0065	–	–	–	–
Standard[a]	1.5	0.0910249 ± 0.0025	0.1515402 ± 0.0056	0.23305 ± 0.0073	0.3194832 ± 0.0065	49.7	55.7	59.7	51.52
6a	10	0.1192428* ± 0.0025	0.1658358* ± 0.0054	0.295185* ± 0.0062	0.3497643* ± 0.0086	34.1	51.5	48.9	46.93
6b	10	0.1057945 ± 0.0056	0.197847 ± 0.0025	0.318536 ± 0.0069	0.3880851 ± 0.0049	41.6	42.2	44.9	41.11
6c	10	0.1663028# ± 0.0026	0.3084498# ± 0.0073	0.53806# ± 0.0036	0.6288178# ± 0.0053	8.12	9.81	6.91	4.58
6d	10	0.1636602 ± 0.0072	0.302499 ± 0.0016	0.495693 ± 0.0014	0.5697055 ± 0.0086	9.58	11.6	14.2	13.55
6e	10	0.1244918 ± 0.0026	0.230679 ± 0.0059	0.374255 ± 0.0051	0.4310519 ± 0.0037	31.2	32.6	35.3	34.59
6f	10	0.1624475 ± 0.0032	0.3023622 ± 0.0026	0.488526 ± 0.0024	0.5695078 ± 0.0094	10.3	11.6	15.5	13.58
6g	10	0.1078036 ± 0.0056	0.201267 ± 0.0046	0.328015 ± 0.0082	0.3763549 ± 0.0086	40.4	41.2	43.3	42.89
6h	10	0.1220302 ± 0.0048	0.2305422 ± 0.0029	0.366741 ± 0.0082	0.4311178 ± 0.0032	32.6	32.6	36.6	34.58
6i	10	0.0957128** ± 0.0026	0.1535238** ± 0.0082	0.241604** ± 0.0052	0.2687402** ± 0.0014	47.1	55.1	58.2	59.22
6j	10	0.1657236 ± 0.0085	0.3062952 ± 0.0046	0.513784 ± 0.0035	0.5916502 ± 0.0025	8.44	10.4	11.1	10.22
6k	10	0.1680223 ± 0.0053	0.3003102 ± 0.0072	0.495808 ± 0.0065	0.5989651 ± 0.0056	7.17	12.2	14.2	9.11
6l	10	0.1114055 ± 0.0045	0.2047896 ± 0.0063	0.328015 ± 0.0058	0.3851196 ± 0.00547	38.5	40.1	43.3	41.56
6m	10	0.1680404 ± 0.0026	0.303867 ± 0.0055	0.499681 ± 0.0095	0.5762296 ± 0.0065	7.16	11.2	13.6	12.56

[a]Values are signified as mean ± S.E.M. (n = 6); data were analysed *via* one-way ANOVA trailed through Dunnett's post hoc tests.
**$p < 0.01$, *$p < 0.05$, #$p > 0.05$ when equated with control group.

donating 4-methoxy substituent, which may improve molecular interactions with the target site. In comparison, the unsubstituted analogue **6a** also demonstrated notable activity, suggesting that substitution on the phenyl ring plays an important role in modulating the anti-inflammatory response (Table-3).

Conclusion

This study established an efficient synthetic route for the phenyl-triazolo-thiadiazole derivatives (**6a-m**) and confirmed their structures using FTIR, NMR, mass spectrometry and elemental analysis. Comprehensive *in silico* evaluations including molecular docking, toxicity prediction, DFT analysis and molecular dynamics simulations, identified ligand **6i** as the most promising candidate. Docking studies demonstrated superior binding affinity and toxicity assessments indicated favourable safety profiles. DFT analysis revealed differences in electronic and stability properties among the derivatives, with **6i** exhibiting moderate electrophilicity and high chemical reactivity, suggesting significant biological potential. MD simulations confirmed the dynamic stability of the ligand-protein complex, supported by consistent RMSD/RMSF values, stable secondary structures and persistent non-covalent interactions. These findings highlight ligand **6i** as a potential lead scaffold for drug development. Further evaluation through biological assays, such as the carrageenan-induced rat paw edema model, along with expanded pharmacokinetic studies and structure-activity relationship analyses, will be essential to advance these derivatives toward therapeutic applications.

ACKNOWLEDGEMENTS

The authors are grateful to the Facilities at Punjab University, Chandigarh (SAIF, CIL, UCIM), for providing the nuclear magnetic resonance (NMR) and mass spectrometry facilities.

CONFLICT OF INTEREST

The authors declare that there is no conflict of interests regarding the publication of this article.

DECLARATION OF AI-ASSISTED TECHNOLOGIES

During the preparation of this manuscript, the authors used an AI-assisted tool(s) to improve the language. The authors reviewed and edited the content and take full responsibility for the published work.

REFERENCES

1. A. Singh, D. Malhotra, K. Singh, R. Chadha and P.M.S. Bedi, *J. Mol. Struct.*, **1266**, 133479 (2022); https://doi.org/10.1016/j.molstruc.2022.133479
2. S.T. Gaballah, H. Amer, A. Hofinger-Horvath, M. Al-Moghazy and M.I. Hemida, *Egypt. J. Chem.*, **63**, 171 (2020); https://doi.org/10.21608/ejchem.2019.13909.1862
3. S. Sharma, M. Devgun, R. Narang, S. Lal and A.C. Rana, *Indian J. Pharm. Educ. Res.*, **56**, 646 (2022); https://doi.org/10.5530/ijper.56.3.113
4. A.F. Kassem, R.H. Althomali, M.M. Anwar and W.I. El-Sofany, *J. Mol. Struct.*, **5**, 1303 (2024); https://doi.org/10.1016/j.molstruc.2024.137510
5. P.M. Jadhav, S. Kantevari, A.B. Tekale, S.V. Bhosale, R.P. Pawar and S.U. Tekale, *Phosphorus Sulfur Silicon Relat. Elem.*, **196**, 879 (2021); https://doi.org/10.1080/10426507.2021.1945601
6. A. Petrou, M. Fesatidou and A. Geronikaki, *Molecules*, **26**, 3166 (2021); https://doi.org/10.3390/molecules26113166
7. I.H. Ripain and N.A. Ngah, *Malays. J. Anal. Sci.*, **25**, 257 (2021).
8. Sahil, K. Kaur and V. Jaitak, V., *Curr. Med. Chem.*, **29**, 4958 (2022); https://doi.org/10.2174/0929867329666220318100019
9. T.A. Farghaly, A.M. Alsaedi, N.A. Alenazi and M.F. Harras, *Expert Opin. Ther. Pat.*, **32**, 791 (2022); https://doi.org/10.1080/13543776.2022.2067477
10. P. Mohanty, S. Behera, R. Behura, L. Shubhadarshinee, P. Mohapatra, A.K. Barick and B.R. Jali, *Biointerface Res. Appl. Chem.*, **12**, 2171 (2021); https://doi.org/10.33263/BRIAC122.21712195
11. P.K. Sharma, A. Amin and M. Kumar, *Open Med. Chem. J.*, **14**, 256 (2020).
12. A. Bhatnagar and G. Pemawat, *Phosphorus Sulfur Silicon Relat. Elem.*, **198**, 554 (2023); https://doi.org/10.1080/10426507.2023.2189253
13. U. Fathy, *J. Sulfur Chem.*, **45**, 786 (2024); https://doi.org/10.1080/17415993.2024.2338270
14. J. Ghanaat, M.A. Khalilzadeh and D. Zareyee, *Mol. Divers.*, **25**, 223 (2021); https://doi.org/10.1007/s11030-020-10050-0
15. A.A. Alexa, V.N. Bercean, S.E. Boncea, A. Ledeti, V. Badea, A. Ridichie, M. Motoc and I. Ledeti, *Appl. Sci.*, **14**, 6180 (2024); https://doi.org/10.3390/app14146180
16. A.A. El-Rashedy, M.N. Yousif, N.E. Ibrahim and M.F. El-Shehry, *Russ. J. Bioorg. Chem.*, **50**, 1583 (2024); https://doi.org/10.1134/S1068162024040022
17. R. Wilcken, M.O. Zimmermann, A. Lange, A.C. Joerger and F.M. Boeckler, *J. Med. Chem.*, **56**, 1363 (2013); https://doi.org/10.1021/jm3012068
18. N.A. Karande and L.G. Rathi, *Indian J. Heterocycl. Chem.*, **30**, 11 (2020).
19. N.A. Karande, L.G. Rathi, K.S. Kamble, A. Nagar, S. Gholve, A.R. Bendale, K. Danao and P.D. Bangre, *Pharm. Chem. J.*, **57**, 234 (2023); https://doi.org/10.1007/s11094-023-02873-6
20. C. Gunaydin and S.S. Bilge, *Eurasian J. Med.*, **50**, 116 (2019); https://doi.org/10.5152/eurasianjmed.2018.0010
21. P.D. Bangre, N.A. Karande, L.G. Rathi, D.J. Singhavi, R.O. Ganjiwale, A. Nagar, A.R. Bendale and K.R. Danao, *Indian J. Heterocycl. Chem.*, **34**, 1 (2024); https://doi.org/10.59467/IJHC.2024.34.1
22. K. Brune and P. Patrignani, *J. Pain Res.*, **8**, 105 (2015); https://doi.org/10.2147/JPR.S75160
23. S. Chahal, P. Rani, Kiran, J. Sindhu, G. Joshi, S. Kalyaanamoorthy, A. Ganesan, Mayank, P. Kumar, R. Singh and A. Negi, *ACS Omega*, **8**, 17446 (2023); https://doi.org/10.1021/acsomega.3c00692
24. OECD, Test No. 420: Acute Oral Toxicity-Fixed Dose Procedure, OECD Guidelines for the Testing of Chemicals, Sec. 4, OECD Publishing, Paris (2002).
25. C.A. Winter, E.A. Risley and G.W. Nuss, *Exp. Biol. Med.*, **111**, 544 (1962); https://doi.org/10.3181/00379727-111-27849